Geometric Dynamic Recrystallization in an AA2219 Alloy Deformed to Large Strains at an Elevated Temperature

R.Kaibyshev[1], I.Mazurina[1], O.Sitdikov[1,2]

[1]Institute for Metals Superplasticity Problems, Khalturina 39, Ufa 450001, Russia

[2]National Institute for Material Science, Sengen 1-2-1, Tsukuba, Ibaraki 305-0047, Japan

Keywords: dynamic recrystallization, thermomechanical processing, equal channel angular extrusion, aluminum alloy, hot deformation

Abstract. The mechanism of new grain evolution during equal channel angular extrusion (ECAE) up to a total strain of ~12 in an Al-Cu-Mn-Zr alloy at a temperature of 475°C ($0.75T_m$) was examined. It was shown that the new grains with an average size of about 15 μm result from a specific process of geometric dynamic recrystallization (GRX) which can be considered as a type of continuous dynamic recrystallization (CDRX). This process involves three elementary mechanisms. At moderate strains, extensive elongation of initial grains takes place; old grain boundaries become progressively serrated. Upon further ECAE processing, transverse low-angle boundaries (LAB) with misorientation ranging from 5 to 15° are evolved between grain boundary irregularities subdividing the initial elongated grains on crystallites with essentially equiaxed shape. The misorientation of these transverse subboundaries rapidly increases with increasing strain, resulting in the formation of true recrystallized grains outlined by high-angle boundaries from all sides. In the same time, the average misorientation of deformation-induced boundaries remains essentially unchanged during ECAE. It is caused by the fact that the evolution of LABs with misorientation less than 4° occurs continuously during severe plastic deformation. The mechanism maintaining the stability of the transverse subboundaries that is a prerequisite condition for their further transformation into high-angle boundaries (HABs) is discussed.

Introduction

There are many potential advantageous in the use of aluminum alloys with fine grains for structural applications. The as-cast grain size of aluminum alloys is generally greater than 100 μm, and grain refinement is achieved by thermomechanical processing routes involving static recrystallizion of a cold or warm worked material or dynamic recrystallization [1]. Recent research works have shown that the application of intense plastic deformation allows achieving an extensive grain refinement in different aluminum alloys [2-5]. Despite much activity in this field, only a limited number of studies were focused on the mechanism of grain refinement during severe plastic deformation [3,4,6,7]. Authors belonging to the Manchester group suggested that the microstructure evolution in aluminum alloys resulting in the grain refinement to the submicron level under ECAE at low temperatures occurs by the extension and compression of initial grain boundaries with strain followed by subdivision of ribbon grain structure by transverse high-angle boundaries (HAB) being formed discontinuously [3,4]. This process, providing a major fraction of the resulting HABs, is often termed GRX [1,8].

Initially, the formation of new grains through GRX was found in pure Al [9] and dilute Al-Mg [1,10,11] subjected to torsion or compression with large strain at T≥400°C. It was suggested that GRX is apparent dynamic recrystallization. Large plastic deformation leads to such extensive elongation of original grains that the size of serrations becomes comparable with the grain thickness. (Fig.1). Next, serrations come into contact resulting in subdivision of flattened initial

grains. Thus, the serrated old boundaries are pinched off providing the formation of new crystallites with equiaxed shape and outlined by HABs from all sides.

It was established that there exist two critical conditions for GRX occurrence [1,8].

(i) Initial grains are deformed as a whole sample; the grain thickness, D, is related to the true strain, ε, and initial grain size, D_o, which can be expressed as

$$\varepsilon=\ln(D_o/D) \quad (1)$$

(ii) The grain thickness, D, has to decrease to a critical value which is of the order of subgrain size, d. It was assumed that the spacing between serrated parts of opposite initial boundaries has to be equal to one [8] or two [9,11] d values allowing the grain boundaries begin locally to come into contact with each other, causing the old grains to pinch off [8]. Therefore, the second necessary condition for GRX is the achievement of the critical strain, ε_{cr}, given as

$$\varepsilon_{cr}=\ln(D_o/d) \quad (2)$$

On the base of experimental results authors [9,11] concluded that a feature of GRX is increasing proportion of HABs with increasing strain due to transition from equiaxed shape of initial grains to plate-like shape. The average misorientation of deformation-induced boundaries remains essentially constant.

The aim of the present study is to establish the mechanism of GRX resulting in grain refinement under severe plastic deformation in an AA2219 alloy at 475°C.

Experimental procedure

The 2219 aluminum alloy with a chemical composition of Al-6.4%Cu-0.3%Mn-0.18%Cr-0.19%Zr-0.06%Fe (in weight pct), denoted as AA2219, was manufactured at the Kaiser Aluminum-Center for Technology by direct chill casting. The AA2219 alloy was subjected to solution treatment at 530°C for 6 hours. Next, the ingot was cooled in air and finally cut into cylinders with 20 mm diameter and 100 mm length. The initial grain size was ~120 μm.

The ECAE pressing was carried out in air using an isothermal die with a circular internal cross-section. The channel had an L-shaped configuration. Deformation through this die produces a strain of ~1 at each passage [2]. Repetitive extrusion up to fixed pressings was used to achieve high strains. Route A in which the specimen is removed from the die and the pressing is repeated without any rotation of the sample [2] was used. The repetitive extrusion was continuously conducted without any intermediate holdings in a furnace. Total time, at which the specimen was held at deformation temperature during ECAE processing, was ~15 min per each extrusion pass. The specimens were water quenched after ECAE pressings to the strains of ~1, ~2, ~4, ~8 and ~12.

Following ECAE, each sample was sectioned parallel to the extrusion direction, and the deformed structure was characterized at the center of the die symmetry plane. Fine structure was examined by TEM. Discs of 3mm diameter were cut from these samples and then ground to a thickness of ~0.25 mm. Next, the discs were electropolished to perforation with a Tenupol–3 twinjet polishing unit using a 20% nitric acid solution in methanol at –32°C and 22 V. Thin foils were examined using a JEOL–2000EX TEM with a double-tilt stage at an accelerating potential of 160 kV. Procedure for estimation of the density of lattice dislocations and technique of optical metallography (OM) were described in early report [12,13] in details.

Misorientation analysis was carried out by the electron back-scattered diffraction (EBSD) technique. For the EBSD analysis, the samples were polished initially using SiC colloid solution. Final electropolishing was carried out in the solution containing 30% HNO_3 and 70%CH_3OH at a temperature of –30°C. The EBSD study was performed using Hitachi S-3500H scanning electron microscopy (SEM) with software TexSem Laboratories, Inc. An area of about 400x150 μm in size was automatically scanned with a 1μm step. (Sub)boundary misorientation distributions were obtained using a software "OIM Analysis 3.0" provided by TexSem Lab., Inc. In the presented data,

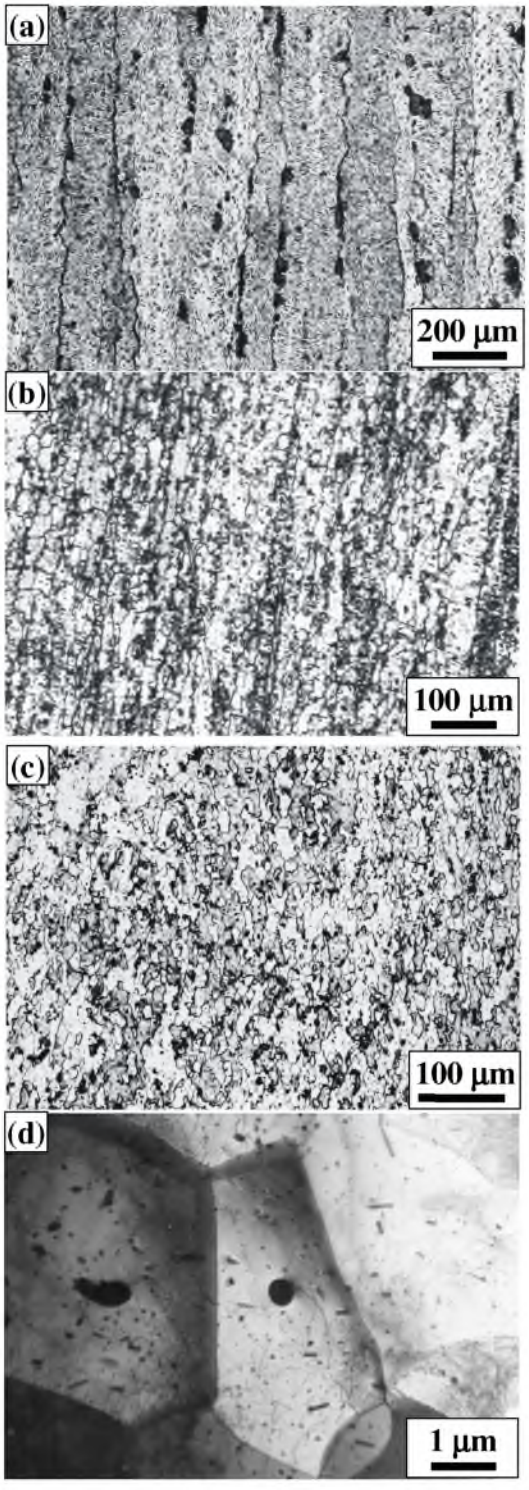

Fig.1. Optical micrographs of AA2219 alloy deformed by ECAE at 475°C to: (a) ε=4, (d) ε=8, (c) ε=12 and (d) TEM micrograph showing the substructure formed in the 2219 Al.

HABs were defined over 15° in misorientation and low-angle boundaries (LAB) as having a misorientation less than 15°. HABs and LABs are depicted in OIM maps as dark and light lines, respectively.

Results

OM studies show that the initial grains elongate in the shear direction at ε≤4; some serration of original boundaries is apparent (Fig.1a). No evidence of grain formation was found at true strains less than ~4 (Fig.1a). Upon further strain chains of new grains located in the shear direction were formed (Fig.1b). Most of these grains exhibit elongated shape, since the equiaxed new grains were also observed. Small areas of new grains alternate with areas of unrecrystallized structure. Notably at ε~8, an extensive serration of old boundaries was found (Fig.1b). After ε~12, a partially recrystallized structure was observed (Fig.1c). However, in comparison with lower strains the recrystallized grains uniformly alternate with unrecrystallized areas. The size of recrystallized grains ranges from 8 to 40 μm. Fine recrystallized grains exhibit an equiaxed shape (Fig.1d), and coarse new grains are elongated in the shear direction. Within the interiors of the last grains arrays of LABs were found.

Observation of fine structure showed that a low density of lattice dislocations ranging from 10^{13} to $5x10^{13}$ m^{-2} took place within the interiors of the (sub)grain (Fig.1d). It is apparent that this density remains essentially unchanged with increasing strain. In particular this density is higher by a factor of about 10 than that observed in a dilute Al-Mg alloys at 450°C under GRX conditions [11,12]. At ε≤2, a poorly defined subgrain structure consisting of separate LABs was found. Three-dimensional arrays of LABs were detected at ε~4. At ε~8, these arrays occupied almost all the unrecrystallized material volume, and at ε~12, mixed arrays consisting of LABs and HABs were evolved (Fig.1d). Thus, ECAE processing leads to an increasing density of deformation-induced boundaries with strain. It is apparent that ε~4 is the inflection point at which a transition from separate LABs to three-dimensional arrays of LABs occurs.

OIM study of samples deformed supports the data of OM and TEM observations. At ε~4, chains of new grain were formed near the initial boundaries (Fig.2a). Notably, orientations of neighbor grains composing these chains are distinctly different (Fig.2a). No chains of elongated new grains with similar orientation were found at this strain. LABs with misorientation over 8° lie in the shear direction in parallel to serrated initial boundaries were

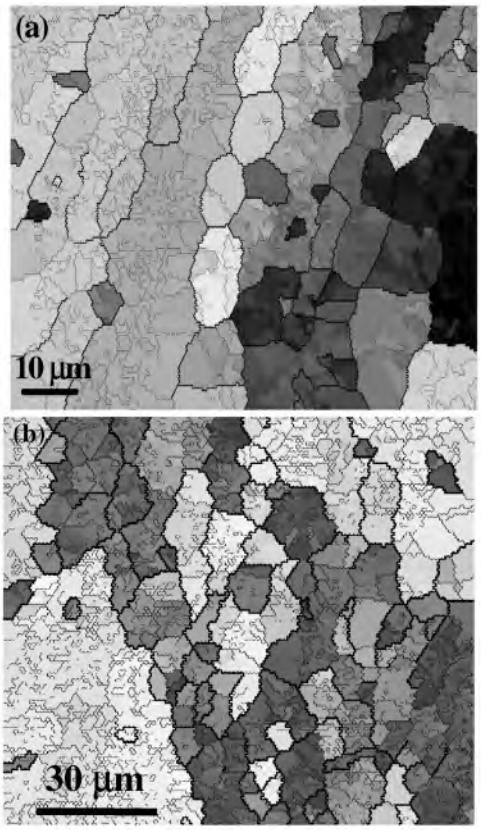

Fig. 2. Orientation imaging microscopy (OIM) maps of the AA2219 alloy deformed by ECAE at 475°C to: (a) ε=8 (b) ε=12.

formed. Isolated segments of these boundaries have high-angle misorientation (Fig. 2a). The formation of transverse LABs with misorientation ranging from 2 to 5° composing three-dimensional arrays was found to occur between extended medium to high-angle boundaries and old grain boundaries. In general, the density of LABs is significantly higher in areas located between these extended boundaries in comparison with the interiors of initial grains. In addition, a well-defined subgrain structure is evolved within recrystallized grains. Upon further strain the number of deformation-induced boundaries within areas locating between initial boundaries or extended medium to high-angle boundaries increases. Chains of fine (sub)grains with essentially similar misorientation were observed after ε~12 (Fig.2b). True recrystallized grains outlined by HABs from all sides are predominant since the fraction of crystallites outlined by HABs and LABs is also significant. The portion of HABs dominates within areas between two initial HABs, whereas LABs is a major fraction within interiors of initial grains. Notably, isolated segments having high-angle origin were observed here.

The evolution of boundary misorientation diagrams with strain is presented in Fig.3. It is seen that the average misorientation remains unchanged with strain. The portion of LABs with misorientation less than 5° is about 60 pct. at all strains examined (Fig. 3a-c). If LABs with $\theta \leq 5^\circ$ were not taken into account (Fig. 3a'-c') the misorientation distribution became distinctly bimodal; the population of HABs tends to minor increase with strain. It is apparent, that LABs with misorientation ranging from 5 to 15° gradually convert to HABs. The density of boundaries with misorientation over 5° increases with increasing strain (Fig.4).

Discussion

In route A of ECAE processing a sample is subjected to alternating strain where deformation takes place in mutually perpendicular directions [14]. Therefore, in this route the initial grains could not become flattened providing the achievement of the second condition for GRX occurrence (Eqs. 2). However, there are three features of microstructure evolution in the AA2219 alloy at 475°C being typical for GRX [1, 11].

(i) The portion of LABs with misorientation less than 2° is high and remains unchanged with strain;
(ii) Average misorientation is essentially constant with strain;
(iii) Chains of recrystallized grains having essentially similar orientation were found at ε~12.

However, there is an ambiguity in the interpretation of these data. The observation of isolated segments of new HABs along continuous LABs and the formation of mixed arrays of low and high-angle boundaries at high strains suggest the operation of CDRX mechanism [1, 15-17] at high temperature. It is known [15-17] that the following main microstructural transformation takes place during CDRX: (i) generation of isolated LABs; (ii) the formation of three-dimensional arrays of LABs; (iii) continuous increase in misorientation of these boundaries resulting in their gradual transformation to HABs. Inspection of experimental data shows that there is a duality in the mechanism of grain refinement. The new grains results from GRX which can be considered as a type of CDRX. At high temperature, in the AA2219 alloy the Al_3Zr nanoscale dispersoids could not play the role of an effective subboundary pinning agent stabilizing the generated LABs with

misorientation less than 2°. Extensive migration of such the LABs results in their collision followed by mutual annihilation of subboundaries consisting of dislocations with opposite Burgers vector [18,19]. Continuous generation and mutual annihilation of LABs with misorientation less than 5° occurring under ECAE processing yield unchanged average misorientiion of deformation-induced boundaries with increasing strain and high population of these boundaries at all strains. A dynamic equilibrium is reached, i.e. the number of generated LABs with $\theta \leq 5^{\circ}$ and the number of annihilated LABs with these misorientations are essentially the same. It is apparent that these LABs are not involved in the process of grain refinement. Generation and annihilation of these LABs is a concomitant process.

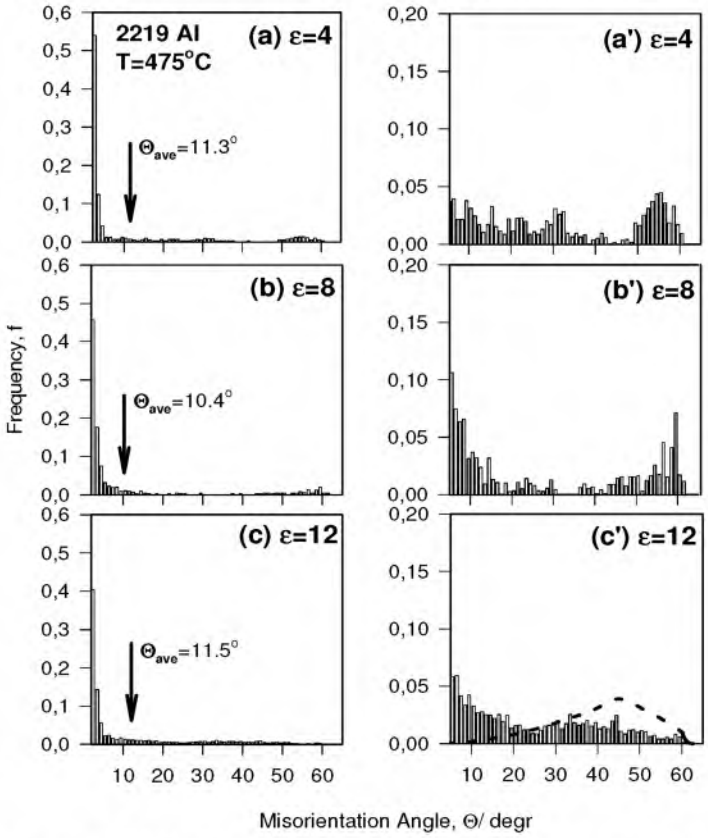

Fig. 3. Misorientation angle distribution in the AA2219 alloy deformed to various strains by ECAE at 475°C

It is obvious that strain-induced continuous reaction can lead to the formation of HABs only if a generated LAB has an ability to increase its misorientation. Therefore, the first stage of CDRX process consists in the formation of immobile LABs, i.e. the generated LABs have to be clamped. It is a prerequisite condition for initiation of CDRX [18] in the AA2219 at 475°C. The clamping of LABs is provided by serrated initial boundaries. The formation of medium to high angle boundaries in the shear direction also plays an important role in stabilization of the LABs. Mechanisms of this clamping are discussed in a parallel issue [20]. Thus, CDRX can occur in the AA2219 alloy at 475°C only within fibrous grains; old grains acquiring flattened shape and the formation of medium to high-angle boundaries parallel to old boundaries create the conditions for CDRX occurrence.

From this point of view the second GRX criterion (Eq. 2) can be reconsidered; a new model for the explanation of this regularity is suggested. It is apparent that serrated initial boundaries can play a role of effective clamping agents stabilizing the LABs evolved within fibrous grains when the spacing between the opposite HABs is equal to two subgrain diameters or less. It seems that transverse LABs are almost immobile owing to the triple junctions between these LABs and serrated old boundaries. As a result, the formation of new grains occurs mainly due to subdivision of the fibrous initial grains. These boundaries trap mobile lattice dislocation that provides their increased misorientation comparing with mobile LABs. Namely immobile LABs convert to HABs with strain.

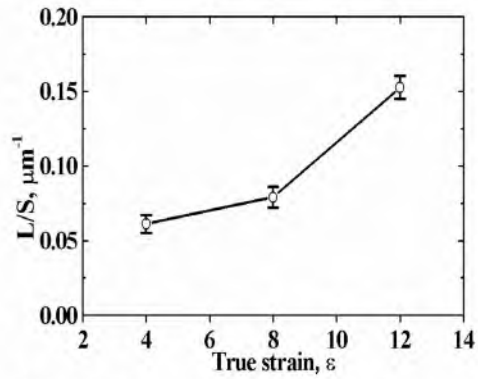

Fig. 4. Strain dependence of boundary density for the AA 2219 alloy deformed by ECAE at 475°C

Upon ECAE processing the density of LABs clamped by serrated old boundaries and deformation-induced medium to high-angle boundaries increases yielding the growth of the grain boundary length per unit volume.

Thus, the mechanism of GRX resulting in grain refinement in the AA2219 under the present conditions consists of three sequential processes.

(i) The formation of band-like structural features. This process involves concurrently the acquirement of flattened shape by initial grains, serration of old grain boundaries and the formation of expanded medium to high-angle boundaries.

(ii) The evolution of immobile LABs within interiors of flattened structural features.

(iii) A gradual increase in misorientation of the immobile LABs resulting in their transformation into HABs.

Acknowledgements

This work was supported in part by the International Science and Technology Center under Project no.2609. The authors would like to thank Dr.A.Goloborodko for carrying out EBSD examinations.

References

[1] F.J.Humphreys, M. Hatherly *Recrystallization and realted annealing phenomena* (Oxford,Pergamon press, 1996),

[2] Y.Iwahashi, Z.Horita, M.Nemoto, T.G. Langdon: Acta Mater., Vol. 46 (1998), p.3317.

[3] F.J. Humphreys, P. B. Prangnell, J. R. Bowen, A. Gholinia, C. Harris: Phil.Trans. R. Soc. Lond., v. 357A (1999), p.1663.

[4] P.J.Apps, J.R.Bowen, P.B.Prangnell: Acta Mater., v.51 (2003) p. 2811.

[5] W.Q.Cao, A.Godfrey, Q.Liu: Mater.Sci.Eng., v.361 (2003) p.9.

[6] S.D.Terhune, D.L. Swisher, K.Oh-ishi, Z.Horita, T.G.Langdon, T.R.McNelley: Metall.Mater.Trans., v.33A (2002) p.2173.

[7] A. Goloborodko, O. Sitdikov, T. Sakai, R. Kaibyshev, H. Miura: Mater. Trans., v.44 (2003) p.766.

[8] A. Gholinia, F.J.Humphreys, P.B.Prangnell: Acta Mater. v.50 (2002) p.4461.

[9] J.K.Solberg, H.J. McQueen, N.Ryum, E.Nes: Phil.Mag., v.60 (1989) p.447.

[10] M.R.Drury, F.J.Humphreys: Acta Metall., v.34 (1986) p.2259.

[11] G.A. Henshall, M.E.Kassner, H.J.McQueen: Metall.Trans. (1992) p.881.

[12] R. Kaibyshev, O. Sitdikov, I. Mazurina, D.R. Lesuer: Mater.Sci.Eng., v.334 (2002) p.113.

[13] O.Sh.Sitdikov, R.O.Kaybyshev, I.M.Safarov, I.A.Mazurina: Phys.Metal.Metall., v.92 (2001) p.270.

[14] Z.Horita, M.Furukawa, M.Nemoto, T.G. Langdon: Mater.Sci.Techn. v.16 (2000) p.1239.

[15] S. Gourdet, F. Montheillet: Mater.Sci.Eng. A283 (2000) p.274.

[16] S. Courdet, F. Montheillet: Acta Mater. 51 (2003) p.2685.

[17] M.R. Barnet, F. Montheillet: Acta Mater. 50 (2002) p.2285.

[18] O. Sitdikov, R. Kaibyshev: Mater.Sci.Eng., v.328 (2002) p.147.

[19] M. Biberger, W. Blum: Phil.Mag.A., v.65 (1992) p.757.

[20] R.Kaibyshev, I.Mazurina: *ibid*